Research Article | Vol. 25, No. 20 | 2 Oct 2017 | OPTICS EXPRESS 24138

Optics EXPRESS

Variable self-powered light detection CMOS chip with real-time adaptive tracking digital output based on a novel on-chip sensor

HongYi Wang,[1,*] Youyou Fan,[1,*] Zhijian Lu,[2] Tao Luo,[2] Houqiang Fu,[2] Hongjiang Song,[2] Yuji Zhao,[2] and Jennifer Blain Christen[2]

[1]*School of Microelectronic, Xi'an Jiaotong University, Xi'an, Shaanxi, 710049, China*
[2]*School of Electrical, Computer and Energy Engineering, Arizona State University, Tempe, Arizona 85287, USA*
**fuu.91.3008@stu.xjtu.edu.cn*

Abstract: This paper provides a solution for a self-powered light direction detection with digitized output. Light direction sensors, energy harvesting photodiodes, real-time adaptive tracking digital output unit and other necessary circuits are integrated on a single chip based on a standard 0.18 μm CMOS process. Light direction sensors proposed have an accuracy of 1.8 degree over a 120 degree range. In order to improve the accuracy, a compensation circuit is presented for photodiodes' forward currents. The actual measurement precision of output is approximately 7 ENOB. Besides that, an adaptive under voltage protection circuit is designed for variable supply power which may undulate with temperature and process.

OCIS codes: (250.0250) Optoelectronics; (040.0040) Detectors.

References and links

1. N. Xie and A. J. P. Theuwissen, "Low-power high-accuracy micro-digital sun sensor by means of a CMOS image sensor," J. Electron. Imaging **22**(3), 3030 (2013).
2. P. Sarkar and S. Chakrabartty, "A compressive piezoelectric front-end circuit for self-powered mechanical impact detectors," in *Circuits and Systems (ISCAS) 2013 IEEE International Symposium* (2013), pp. 2207–2210.
3. M. Guan and W. H. Liao, "Comparative analysis of piezoelectric power harvesting circuits for rechargeable batteries Information Acquisition," in *2005 IEEE International Conference* (2005), pp. 243–246.
4. Z. Dong, Y. Wen, H. Liao, and Z. Wen, "Power self-regulation circuit of piezoelectric multi-shaker micro-generator Electronic Measurement and Instruments," in *8th International Conference 2007 ICEMI 07* (2007), pp. 656–660.
5. D. Welch and J. B. Christen, "MEMS optical position sensor for sun tracking," in *2015 IEEE International Symposium on Circuits and Systems* (2015), pp. 1874–1878.
6. P. N. Patil, M. A. Khandekar, and S. N. Patil, "Automatic dual-axis solar tracking system for parabolic dish," in *2016 International Conference on Advances in Electrical, Electronics, Information, Communication and Bio-Informatics*, 2016.
7. J. Quero, A. Guerrero, L. Franquelo, M. Dominguez, I. Ameijeiras, and L. Castaner, "Light source position microsensor Circuits and Systems," in *2001 IEEE International Symposium* (2001), pp. 648–651.
8. K. Karimov, M. Saqib, P. Akhter, M. Ahmed, J. Chattha, and S. Yousafzai, "A simple photo-voltaic tracking system," Sol. Energy Mater. Sol. Cells **87**(1), 49–59 (2005).
9. H. Mousazadeh, A. Keyhani, A. Javadi, H. Mobli, K. Abrinia, and A. Sharifi, "A review of principle and sun-tracking methods for maximizing solar systems output," Renew. Sustain. Energy Rev. **13**(8), 1800–1818 (2009).
10. H. Wang, T. Luo, Y. Fan, Z. Lu, H. Song, and J. B. Christen, "A self-powered single-axis maximum power direction tracking system with an on-chip sensor," Sol. Energy **112**, 100–107 (2015).
11. P. Ortega, G. LoPez-Rodri Guez, J. Ricart, M. Domínguez, L. M. Castañer, J. M. Quero, C. L. Tarrida, J. García, M. Reina, A. Gras, and M. Angulo, "A Miniaturized Two Axis Sun Sensor for Attitude Control of Nano-Satellites," IEEE Sens. J. **10**(10), 1623–1632 (2010).
12. F. J. Delgado, J. M. Quero, J. Garcia, C. L. Tarrida, P. R. Ortega, and S. Bermejo, "Accurate and Wide-Field-ofView MEMS-Based Sun Sensor for Industrial Applications," IEEE Trans. Ind. Electron. **59**(12), 4871–4880 (2012).

1. Introduction

Attitude sensors are widely used in the aircraft's orientation which usually depends on some reference vectors. According to the reference vectors they use, attitude sensors are classified

#301338 https://doi.org/10.1364/OE.25.024138
Journal © 2017 Received 29 Jun 2017; accepted 17 Sep 2017; published 22 Sep 2017
Corrected: 26 September 2017

Optics EXPRESS

into different categories including gyrocompasses, magnetometers, star tracking sensors, and sun tracking sensors. Sun tracking sensors are characterized among the attitude sensors due to their simple structures, low power consumption and low cost in the aircraft applications. In recent years, nanosatellites have rapidly developed in military and commercial field because of nanosatellites' low power consumption, low weight and low cost. A nanosatellite usually has a weight less than 10 kg. So it is significant for the sun tracking sensors which are a necessary part of nanosatellites to minimize. Many kinds of sun sensors have been utilized into space applications including positioning solar panels, orienting solar thermal collectors, and the spacecraft attitude determination [1]. However, most solutions need some special process, such as MEMS, or other off-chip devices which is a trade-off of the weight and size of sensor [2–6]. In this case, it is better to have an on-chip light direction sensor for this system. Many techniques have been developed to detect light direction, such as the shading device method [7], the tilted surface method [8], and the collimator tube method [9]. However, this conventional techniques have some disadvantages on accuracy, size and integration [10]. Both small form factor and low power consumption is required by many aircraft applications. Since we can use the light detected to provide needed energy, energy harvesting is an attractive approach which absorbs ambient energy to support the system. A self-powered on-chip sensor is a smart choice to meet these requirements. Some complete solutions have been presented, but these solutions just offer an analog output which cannot directly provide control signals to the system [11, 12] e.g., controlling attitude of solar panel or aircraft. This paper demonstrates a self-powered solution with an on-chip light direction sensor and real-time adaptive tracking digital output solution to detect the direction of the incident light. In our approach, the integrated real-time adaptive tracking digital output unit can generate a digitized output that can directly control the system. Built-in photodiodes are utilized to harvest energy so no external power supply is needed when the chip works. On-chip photo sensor offers the light direction with an accuracy of 1.8 degree over a 120 degree range. In addition, the digitized output has an accuracy of approximate 7 ENOB (Efficient Number Of Bits).

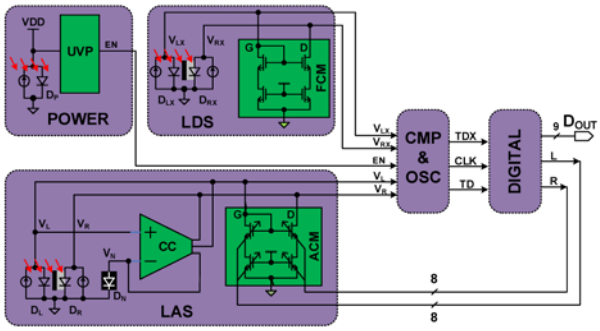

Fig. 1. The block diagram of the self-powered light direction chip.

2. Top-level Design

The complete block diagram of the self-powered sensor chip we presented in this work is shown in Fig. 1 including five blocks: POWER, LDS, LAS, OSC & CMP and DIGITAL. In POWER block, the photodiode DP harvests energy for the other blocks. The current sources beside diodes indicate the photocurrents generated by corresponding photodiodes. Under Voltage Protection (UVP) is an adaptive supply voltage monitoring circuit. When VDD is lower than the threshold of transistor which changes due to process deviation, the circuit provides an EPN signal to switch the chip into sleep mode in which oscillator stops but the digitized output is stored to decrease the power consumption. LAS is a Light Angle Sensor with the Adjustable Current Mirror (ACM) which is regulated by the further digitized signals

Optics EXPRESS

and LDS is a Light Direction Sensor with the Fixed Current Mirror (FCM). Two identical photodiodes are located on opposite sides of the micro-scale metal wall as it is revealed in both LAS and LDS. The four identical photodiodes D_L, D_{LX}, D_R, and D_{RX} generate four different photocurrents with diverse incident light. Current mirror ACM and FCM convert the four photocurrents into four voltage signals V_L, V_{LX}, V_R and V_{RX}. These signals come into OSC & CMP block to generate direction and angle signals TDX and TD. Besides that, the OSC & CMP block also generates clock signal CLK. Depending on these signals, DIGITAL block produces two 8 bits digitized signals to adjust the ratio of the current mirror ACM and a 9 bits digitized signal for incident light information. In order to improve the measurement precision, a Current Compensation (CC) circuit is designed in LAS. These blocks will be described in detail in the latter parts of this paper. Section 3 describes the photo sensor and the circuit implement of proposed approach. Section 4 gives the measure results and discussion. Finally, conclusions are presented in Section 5.

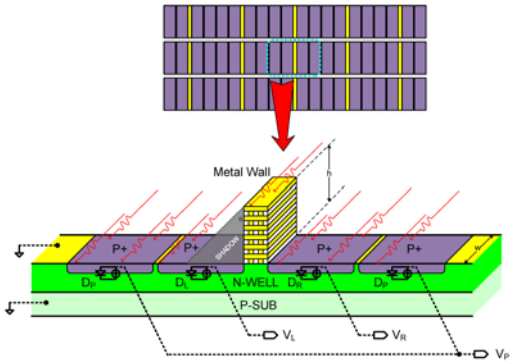

Fig. 2. Structure of the presented on-chip sensor.

3. Circuit Implementation

3.1 Photo Sensor

Figure 2 shows the structure of the on-chip light direction sensor, the diodes pairs D_L, D_{LX}, D_R, and D_{RX} have the same structure. The basic sensor cell of the on-chip light direction sensor lies in the right of Fig. 1. A number of basic sensor cells form the on-chip light direction sensor shown in the left. As an innovative detection method, the sensor we presented consists of 154 individual sensor basic cells for a total area of approximately 1.25 mm^2 fabricated in a standard 0.18 μm CMOS process. Each cell has a metal wall created by stacking all metal layers, contacts, and vias available in the process to generate on-chip micro-scale shadow. The height of the metal wall is h, and the width of identical photodiodes on both sides of the wall is w. We should optimize the dimensions of the metal wall for the sensors good performance. In this design, diffraction has also been considered. As we all know, the bandgap voltage of silicon is about 1.12 V. So the longest wavelength of the absorbed light is about 1.1 μm, actually the absorption peak is around 0.7 μm. In this design, height is designed as 12 μm and width is designed ad 15 μm. The physical dimensions are much larger than the wavelength of the absorbed light. So the diffraction has little influence on the sensors performance. The basic cell of the photodiode is built by P + resistance in N-well. The contact of the N-well and the connection metals form a wall which is used to block the light pass through the middle position of the two photodiodes. When the light comes from not just the middle top, the two photodiodes will receive different luminous flux, hence the two photodiodes generate different amount of currents. As it is shown in Fig. 2, light comes from right to left and this means the right photodiode is fully illuminated and the left one is partly shadowed by the metal wall. In this case, the total photocurrent generated by the right

Optics EXPRESS

diode D_R can be divided into three parts. The first part of the current is the current generated by the light which directly illuminates the diode. The second part is the current generated by the reflected light from the metal wall. And the rest of the current is generated by the residual light reflected many times by the back metal base, the metal layers, and the interfaces of different materials. For the left photodiode DL, the total current consists of only the first and the third part. So the expressions of photodiodes currents and incident light can be derived as following. As we known, the photocurrent generated by a photodiode is proportional to the optical power the photodiode receives. The short-circuit photocurrent can be written as Eq. (1):

$$I_{DIO} = kP_T = kP_0 A_{EFF} = kP_0 w L_{EFF} \tag{1}$$

where, k is a constant coefficient, P_T is the total optical power the diode receives, P_0 is the optical power per unity sectional area of the light, A_{EFF} is the sectional area of the incident light, and L_{EFF} is the length of the sectional area. As it is mentioned above, we can give the expressions of three parts of currents according to Eq. (1) and the sensor structure. Here, we define as the angle between mental wall and incident light direction. The first part current is shown as Eq. (2).

$$I_{LDirection} = kP_0 wl \sin\theta \tag{2}$$

The second part of current is the current generated by the reflected light from the metal wall. So we assume the ratio of the light reflected to the total light reaching the right side of the metal wall is because the light comes from right to left. This part of photocurrent is described as

$$I_{\mathrm{Re}\,flection} = kP_0 wh \sin\theta \tag{3}$$

The third part of the photocurrent can be thought as the sum of all those currents produced by these background lights. So this part of current can be indicated as

$$I_{LBackground} = \beta kP_0 wl \sin\theta \tag{4}$$

Where, β is other constant in this equation.

In this case, the currents generated by D_R contain three parts of currents. And photodiode D_L does not provides $I_{LReflection}$ due to shadow. The total currents of photodiodes D_R and D_L are expressed in Eqs. (5) and (6), respectively.

$$I_{PR} = kP_0 w\left[(1+\beta) l\cos\theta + \alpha h \sin\theta\right] \tag{5}$$

$$I_{PL} = kP_0 w\left[(1+\beta) l\cos\theta - h \sin\theta\right] \tag{6}$$

The ratio of I_{PR} and I_{PL} has been shown in Eq. (7), and the incident light angle can be described by the photodiode currents ratio. From Eq. (7), the relationship of current ratio and incident light angle can be determined in some a design. Because w and l are constants when the device has been fabricated. The coefficient and depend on the process, layout and package which are also constants in our design.

$$\frac{I_{PR}}{I_{PL}} = \frac{(1+\beta) l\cos\theta + \alpha h \sin\theta}{(1+\beta) l\cos\theta - h \sin\theta} \tag{7}$$

In this case above, a function of the ratio of current and the incident light angle has been derived when light comes from right to left. When light comes from left to right, we can get a similar function as Eq. (8). Therefore, from Eq. (8) we can see the current ratio of IL/IR is independent on the light intensity and only depends on the incident light angle.

$$\frac{I_{PR}}{I_{PL}} = \frac{(1+\beta) l\cos\theta + h \sin\theta}{(1+\beta) l\cos\theta - \alpha h \sin\theta} \tag{8}$$

Optics EXPRESS

The photodiode model shown in Fig. 2 is composed of a current source and a diode. D_R and D_L which locate on both of the metal baffle are utilized to detect light. Two energy harvesting photodiodes D_P placed separately on both sides of the sensor cell are used to provide power for the whole chip. The photocurrent ratio of the smaller one to the larger one in D_R and D_L is almost linearly dependent on the angle of the incident light. A function of the ratio of current and the incident light angle has been described above. According to the function, we can get the incident light angle messages with an accuracy of 1.8 degrees over a 120 degree range.

3.2 Forward Current Compensation Circuit

The current ratio of the two photodiodes D_L and D_R shown in Fig. 3 has an approximate linear relationship with the angle of the incident light. As described above, we use a basic model for the photodiodes composed of a diode and a current source, the forward currents I_{DL} and I_{DR} decrease the accuracy of the ratio between two photocurrents. So we present a compensation circuit (CC) as shown in Fig. 3 to compensate the forward current. In this circuit, we design a special diode D_N which is the same kind of D_L and D_R but is completely shielded by metal layers, thus there is no photocurrent in D_N. The size ratio of D_N, D_L, D_R is 1: n: n. In order to match the current, PMOS currents has the same ratio of 1: n: n. The NMOS threshold voltage in this process is about 0.3 V. The voltages V_L and V_R will be higher than the NMOS threshold voltage when the photocurrents I_{PL} and I_{PR} flow through ACM. If I_O is low, D_N is reverse biased and V_N is low. While V_L is about NMOS threshold voltage 0.3 V, because there is a photocurrent flowing I_{PL} into the ACM. If I_O is high, D_N is forward biased and V_N is about 0.6 V. The V-I curves of the diode D_N and photodiode D_L has been described in the lower right corner of Fig. 3. The curves describe the relationship of voltage between D_N and DL in different current conditions. The OP shown in the yellow part of Fig. 3 is used to keep $V_N = V_L$. Based on Kirchhoff's Current Law at the point A, we can get the equation as follow: $nI_O + I_{PL} = I_{DL} + I_L$. Considering the size ratio of diodes, $I_{DL} = nI_{PN} = nI_O$. Hence, we can get another equation $I_{PL} = I_L$ which means that all the photocurrents generated by DL flow into ACM without the effect of forward currents. For I_{PR}, when the real-time adaptive tracking digital output unit reaches a balanced state, V_R almost equals to V_L, so $I_{DR} = nI_{DL} = nI_O$, and hence $I_{PR} = I_R$. So the compensation circuit works well and enhances the accuracy of the ratio between two photocurrents.

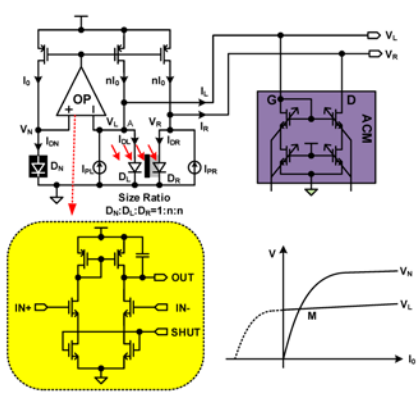

Fig. 3. Forward current IDL and IDR compensation circuit.

3.3 OSC & CMP Block

The OSC & CMP block shown in Fig. 4 generates incident light angle/direction signal TD/TDX and clock signal for DIGTIAL block further processing. It is mentioned above that the photocurrents have been converted into voltages (VL, VLX, VR and VRX) by adjustable

Optics EXPRESS

current mirror (ACM) and fixed current mirror (FCM). These voltages are compared by CMP in OSC & CMP block to get TD and TDX. The comparator has an enable signal SET to control it. Its outputs are both high levels when SET is low. When SET is high, it compares the two input signals VL, VLX, VR and VRX. When the comparing is completed, one of the outputs signal will change to low level. This change will be detected and used to generate the clock signal and to indicate the comparing result. The purple part in Fig. 4 receives the signal SET and outputs XCK with inverse phase after a delay time. So the function of this block can be seen as an inverter. Then we get the clock signal CLK and it is the inverse phase of XCK. Unlike a usual oscillator, the frequency of our oscillator in this work is variable and adaptive. Because the power supply is offered by the photodiode DP absorbing ambient energy which is very limited and varying with the incident optical intensity. So we present a low power digital output unit with an adaptive frequency oscillator to fit the power supply. When the incident optical power is intense, the oscillator will generate high frequency to fit the quick digitized output. On the contrary, the weak power results in the low frequency to decrease the power consumption. The delay time in the oscillator loop depends on not only the comparator operating speed, but also the capacitor values and charging/discharging currents. The T-ADJ block in this work is designed to control the discharging current for adjusting the delay time. It can be seen that the discharging current is dependent on G1 and G2 which are controlled by V_L, V_{LX}, V_R and V_{RX}. The higher incident optical power leads to higher voltages of V_L, V_{LX}, V_R and V_{RX} which results in higher discharging currents in the T-ADJ block. The oscillator outputs a high frequency signal in this condition. Whereas, lower incident optical power results in lower voltages, lower discharging currents and lower frequency finally. T-ADJ block also has a control terminal G3 to enhance the discharging current as necessary. The OSC & CMP block provides CLK, TD, TDX signals which represent clock, light angle and light direction to the DIGITAL block for data processing.

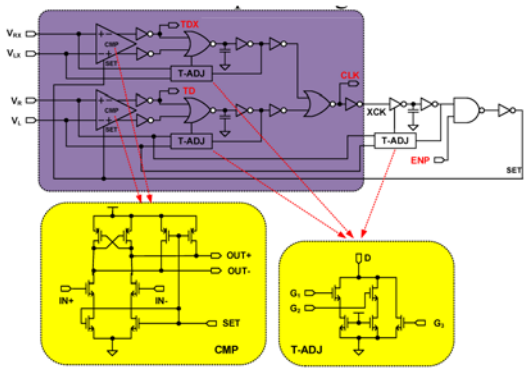

Fig. 4. The schematic of CMP&OSC block.

3.4 Digital Block

DIGITAL block works like an analog to digital converter to generate a 9-bits digitized output. And this digital output unit has an adaptive conversion speed with variable supply power. This block receives three signals TD, TDX and CLK which are generated by OSC & CMP block and outputs three signals L, R and D_{OUT}. L and R both are 8 bits signals which go back to control the current mirror ratio in ACM. D_{OUT} is a 9 bits signal that carries the incident light angle and direction. The first bit of D_{OUT} means the incident light direction left/right with 0/1, respectively. When D_{OUT} begins with 0, it means the light comes from left side, and the other bits of D_{OUT} mean the current ratio of left side to right side. Similarly, D_{OUT} indicates the incident light from right side and the current ratio of right side to left side when the first bit of D_{OUT} is 1. Figure 5 shows the complete block diagram of DIGITAL in this work. DIGITAL block can be divided into three parts, 8 bits up/down adder and register

Optics EXPRESS

circuit, ADD/SUB control signal detection and generation circuit, and output level circuit. The core of DIGITAL block is the 8 bits up/down adder and register circuit which consists of an 8 bits full adder as function of real-time adaptive tracking digital output unit and 8 DFF for latching data. The ADD and SUB signals are generated by all 0 detection circuit and all 1 detection circuit which is shown in the red dotted frame. The two signals are used to control an 8 bits full adder in an add operation or a subtraction operation. When the detected signal D which represents the latter 8 bits of D_{OUT} indicating the current ratio is 00000000, the ADD signal will be 0 and the SUB signal will be 1. So the 8 bits full adder is set to an add operation and D will accumulate. When the signal D is detected as 11111111, the 8 bits full adder will work in subtraction operation and D will decrease. If D is neither 00000000 nor 11111111, the operation mode of full adder will be dependent on TD and TDX rather than ADD and SUB. Not only the full adder but also the Light Angle Output depends on TD. TD and TDX which produced by OSC & CMP block can be permuted and combined into four types 00, 01, 10, and 11. When the combination of TD and TDX is 00 or 11, the full adder will work in a subtraction operation and D decreases. Conversely, when the combination of TD and TDX is 01 or 10, the full adder will work in an add operation and D accumulates. Through output level circuit, we obtain the output D_{OUT}, L and R in different conditions according to TD and TDX. The 8 bits signal L and R which represent the incident light angle information come back to control the adjustable current mirror. Then the adjustable current mirror's outputs change and TD maybe change or not. So D will increase or decrease with the incident light angle changing.

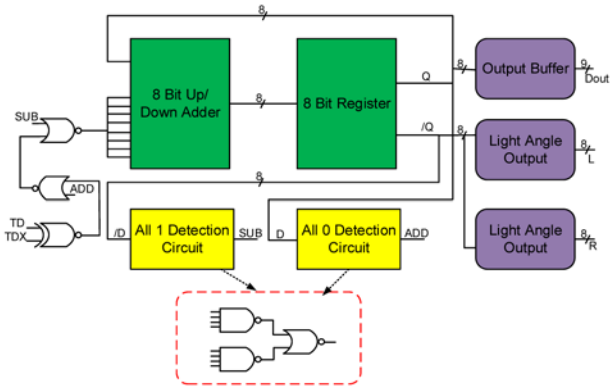

Fig. 5. The diagram block of DIGITAL block for data processing.

3.5 Under Voltage Protection Block

In this work we use photodiodes absorbing ambient light to provide the power supply, however the variable incident optical power leads to unstable power supply. Considering the risk of low supply voltage, an Under Voltage Protection (UVP) circuit is needed. Under Voltage Protection (UVP) as shown in Fig. 6 is designed like a simple power management to detect the voltage of the power supply. VDD is compared with the threshold of transistor not with some a fixed value. So the UVP circuit is adaptive, because the threshold of transistor varieties due to different processes, process deviation or some other environment effects. If the power supply voltage generated by photodiodes is lower than the threshold voltage, the UVP circuit outputs an ENP signal which controls the oscillator entering sleep state and no longer oscillating. In this case, all the digitized outputs are stored and VDD will not decrease more. When the photodiodes harvest enough energy, VDD becomes higher and chip works again. In Fig. 6, there are two resistances which are used to set a threshold range for preventing the ENP signal flipping back and forth. In this work, the wake-up voltage is 383 mV while the standby voltage is 360 mV.

Optics EXPRESS

4. Layout And Test Result

The chip is fabricated in a 0.18 μm CMOS process with 6 metal layers and the whole areas is 4.5 mm^2. Figure 7 shows the micrograph of the test chip including an expanded view of the interface circuits and sensor elements. The interface circuits are covered by metal layers to prevent the circuits from the incident light.

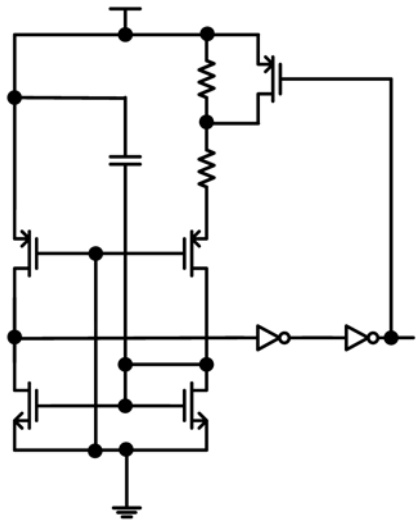

Fig. 6. The schematic of Under Voltage Protection circuit.

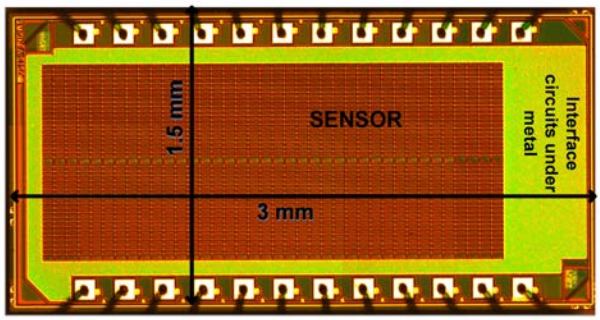

Fig. 7. The micrograph of the self-powered chip.

To verify the performance of our chip, we set up a test platform as shown in Fig. 8. The self-power chip is mounted on a breadboard which is placed on an angular actuator to allow us to adjust the angle of the incident light. We measure the data with an oscilloscope both inside the laboratory and outside under the sun. The energy harvesting photodiodes absorb the ambient light to generate a supply power ranging from 380 mV to 480 mV over the optical intensity from 45 mW/cm^2 to 95 mW/cm^2. In the range of the optical intensity, the chip generates a variable frequency changing from 1.57 kHz to 32.93 kHz. The UVP circuit works and the oscillator stops when the power supply is lower than the threshold approximately 380 mV. Some relationships of VDD and oscillator frequency is shown in Fig. 9. In Fig. 9, it is clear that 380 mV is the minimum evoke voltage and the oscillator frequency changes automatically as VDD varieties. The power supply and frequency are proportional to the optical intensity.

Optics EXPRESS

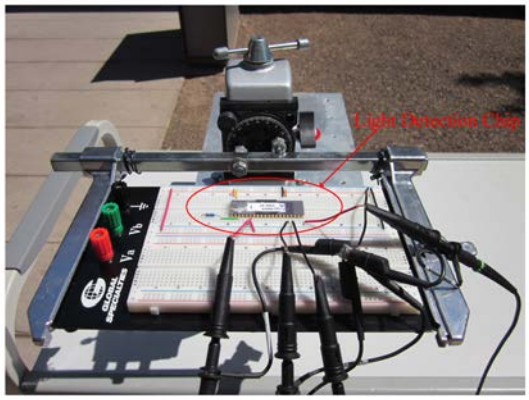

Fig. 8. The test platform of chip.

We adjust the incident light angle to measure the short currents IPR and IPL for an optical intensity of 80 mW/cm^2 as shown in Fig. 10. When the incident light angle is zero, the two photocurrents are equal. When the incident light angle is negative, the left photocurrent is larger than the right one and vice versa. It is significant to calculate a ratio of the small current to the large current for comparison. The calculated ratio will be compared with the digitized output ratio of real-time adaptive tracking digital output and the comparison result has been shown in Fig. 11. The two ratio are very close to each other, and 7 ENOB is achieved as the test results. The power supply is completely driven by on-chip photodiodes without any exterior energy sources. So the power consumption is low ranging from 727 nW to 2.32 μW for the test optical intensity.

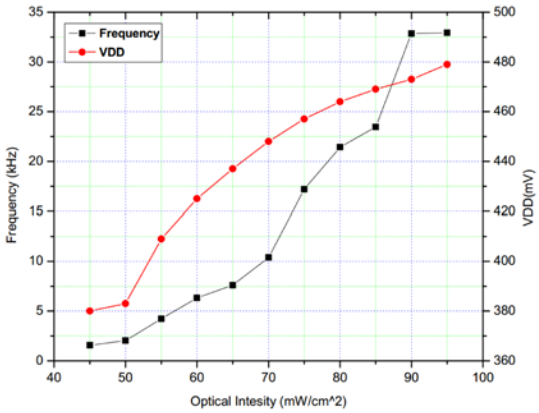

Fig. 9. The relationships of VDD and frequency versus optical intensity.

5. Summary

Based on a 0.18 μm CMOS process, a self-powered real time adaptive tracking digital output solution with photo sensors and necessary circuits for detecting the incident light direction and angle is implemented entirely. The on-chip photodiodes absorb the light energy to provide supply power for the chip. The self-powered chip gives a 9 bits digitalized output D_{OUT} which includes the incident light direction and angle messages. Considering the light sensors noise, the actual measurement precision of output is approximately 7 ENOB lower than the designed target. The supply power varying from 380 mV to 480 mV over the optical intensity from 45 mV/cm^2 to 95 mV/cm^2 results in the variable real-time adaptive tracking digital output conversion speed. The self-powered real-time adaptive tracking digital output

Optics EXPRESS

circuit works at an adjustable speed based on the supply power. For the reliability of the chip, we design an Under Voltage Protection (UVP) circuit. The circuit controls the chip from operation mode to sleep mode when the supply power is lower than 380 mV. The self-powered chip we presented gives a complete solution for light detecting and solar tracking without any other energy.

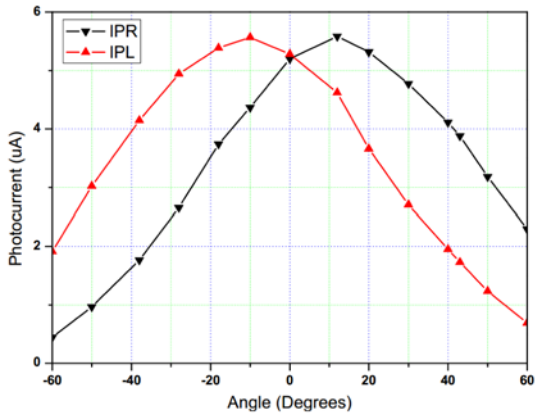

Fig. 10. The relationship of incident light angle with the photocurrent and current ratio

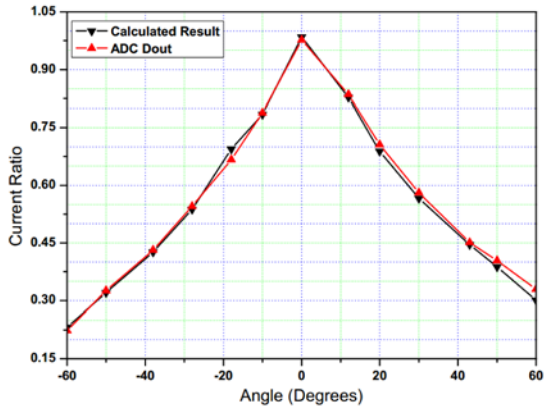

Fig. 11. The comparison of the calculated ratio and the digitized output ratio

Acknowledgement

This research is supported by the National Natural Science Foundations of China under grants 60806009 and 11271297, and the MOSIS Educational Program. This research is also supported by the Basic science research plan of Shaanxi Province (2015JM6358) and the Fundamental Research Funds for the Central Universities (xjj2014120).